Probabilistic Initial Orbit Determination From Radio Frequency Measurements Using Gaussian Mixture

Andrew J. Sinclair
Air Force Research Laboratory
Edwin G. W. Peters
The University of New South Wales Canberra

Joseph T. A. Peterson
Texas A&M University

Melrose Brown
The University of New South Wales Canberra

1. INTRODUCTION

Radio frequency (RF) observations are an attractive source for characterization of transmitting satellites. For purposes of orbit determination, relevant RF measurements include time difference of arrival (TDOA) and frequency difference of arrival (FDOA). TDOA measurements are related to the difference in range from the transmitter to two receivers. FOA measurements are related to the range rate from the transmitter to each receiver. Extensive work in the literature has developed signal processing methods to extract these measurements from received RF signals [1, 2]. These types of measurements have been broadly studied for the purposes of geolocation [3–7]. The use of these measurements for orbit determination has also been considered [8–10]. These studies have fallen into two categories: initial orbit determination without full characterization of probability density function of the state, or iterative refinement of a current estimate or initial guess.

This paper addresses initial orbit determination using TDOA and FOA or FDOA measurements with no a priori knowledge of the transmitter's orbit. An initial set of a TDOA measurement and frequency measurements leaves a manifold in the six-dimensional state space of the transmitter's orbit over which the probability distribution is assumed to be uniform. In the position space, the uniform distribution is supported on the hyperboloid defined by the TDOA measurement with the receivers at the foci. For a given position, the frequency measurements leave a uniform distribution over certain components of the transmitter's velocity. This distribution is approximated via Gaussian mixture (GM) using Cartesian coordinates of the transmitter's position and velocity. The use of GM approximation is similar to Reference [6], but that work focused on tracking of terrestrial emitters. The use of GM for probabilistic initial orbit determination using angles-only observations was introduced by DeMars & Jah [11].

The remainder of the paper is organized as follows. Section 2 describes the TDOA, FOA, and FDOA measurements and their Jacobians. Section 3 describes how the probability density resulting from an underdetermined set of measurements can be modeled as a uniform-Gaussian distribution. Sections 4-7 develop GM approximations for the uniform distributions in the position and velocity space separately. These distributions are combined to create the GM approximation of the uniform-Gaussian distribution of the orbital state in Section 8. Section 9 describes the incorporation of subsequent measurements via a GM extended Kalman filter. A numerical example and concluding remarks are provided in Sections 10 and 11, respectively.

2. MEASUREMENT MODEL

A time difference of arrival (TDOA) measurement relates the arrival times of a transmitted signal at two different receivers. This TDOA is related by the speed of light to the difference in range from the transmitter to each receiver.

$$\Delta r = r_{t,2} - r_{t,1} = \sqrt{(\boldsymbol{r}-\boldsymbol{r}_2)^{\mathsf{T}}(\boldsymbol{r}-\boldsymbol{r}_2)} - \sqrt{(\boldsymbol{r}-\boldsymbol{r}_1)^{\mathsf{T}}(\boldsymbol{r}-\boldsymbol{r}_1)} \tag{1}$$

Here, $\boldsymbol{r}$ is the unknown position of the transmitter, and $\boldsymbol{r}_1$ and $\boldsymbol{r}_2$ are the known positions of the two receivers. A noise-free TDOA measurement places the transmitter on one sheet of a two-sheeted hyperboloid with the receivers at the foci.

The frequency of arrival (FOA) at each receiver is related to the Doppler shift due to the range rate from the transmitter to each receiver. For a continuous wave of a single frequency, measuring the received frequencies does not allow for solution of the range rates and the unknown transmit frequency. However, some knowledge about the frequency content of the signal allows for solution of the range rates.

$$\dot{r}_{t,i} = \frac{(\boldsymbol{r}-\boldsymbol{r}_i)^{\mathsf{T}}(\boldsymbol{v}-\boldsymbol{v}_i)}{\sqrt{(\boldsymbol{r}-\boldsymbol{r}_i)^{\mathsf{T}}(\boldsymbol{r}-\boldsymbol{r}_i)}} \qquad \text{for } i = 1,2 \tag{2}$$

Here, $\boldsymbol{v}$ is the unknown velocity of the transmitter, and $\boldsymbol{v}_i$ is the known velocity of the ith receiver.

Alternatively, a frequency difference of arrival (FDOA) measurement is related to the difference in range rate from the transmitter to each receiver.

$$\Delta\dot{r} = \dot{r}_{t,2} - \dot{r}_{t,1} = \frac{(\boldsymbol{r}-\boldsymbol{r}_2)^{\mathsf{T}}(\boldsymbol{v}-\boldsymbol{v}_2)}{\sqrt{(\boldsymbol{r}-\boldsymbol{r}_2)^{\mathsf{T}}(\boldsymbol{r}-\boldsymbol{r}_2)}} - \frac{(\boldsymbol{r}-\boldsymbol{r}_1)^{\mathsf{T}}(\boldsymbol{v}-\boldsymbol{v}_1)}{\sqrt{(\boldsymbol{r}-\boldsymbol{r}_1)^{\mathsf{T}}(\boldsymbol{r}-\boldsymbol{r}_1)}} \tag{3}$$

The measurement vector $\boldsymbol{y}$ is formed subject to additive, Gaussian noise $\boldsymbol{w}$ with zero mean and covariance matrix $\boldsymbol{R}$. For the case of TDOA and FOA measurements, the measurement vector has the following form.

$$\boldsymbol{y} = \begin{bmatrix} \Delta r \\ \dot{r}_{t,1} \\ \dot{r}_{t,2} \end{bmatrix} + \boldsymbol{w} \tag{4}$$

Defining the orbital state $\boldsymbol{x} = [\boldsymbol{r}^{\mathsf{T}}\ \boldsymbol{v}^{\mathsf{T}}]^{\mathsf{T}}$, the measurement Jacobian can be evaluated.

$$\boldsymbol{H} \equiv \frac{\partial \boldsymbol{y}}{\partial \boldsymbol{x}} = \begin{bmatrix} \boldsymbol{H}_{\Delta r,r} & \boldsymbol{0} \\ \boldsymbol{H}_{\dot{r},r} & \boldsymbol{H}_{\dot{r},v} \end{bmatrix} = \begin{bmatrix} \frac{(\boldsymbol{r}-\boldsymbol{r}_2)^{\mathsf{T}}}{\sqrt{(\boldsymbol{r}-\boldsymbol{r}_2)^{\mathsf{T}}(\boldsymbol{r}-\boldsymbol{r}_2)}} - \frac{(\boldsymbol{r}-\boldsymbol{r}_1)^{\mathsf{T}}}{\sqrt{(\boldsymbol{r}-\boldsymbol{r}_1)^{\mathsf{T}}(\boldsymbol{r}-\boldsymbol{r}_1)}} & \boldsymbol{0} \\ \frac{(\boldsymbol{v}-\boldsymbol{v}_1)^{\mathsf{T}}}{\sqrt{(\boldsymbol{r}-\boldsymbol{r}_1)^{\mathsf{T}}(\boldsymbol{r}-\boldsymbol{r}_1)}} - \frac{(\boldsymbol{r}-\boldsymbol{r}_1)^{\mathsf{T}}(\boldsymbol{v}-\boldsymbol{v}_1)(\boldsymbol{r}-\boldsymbol{r}_1)^{\mathsf{T}}}{\left((\boldsymbol{r}-\boldsymbol{r}_1)^{\mathsf{T}}(\boldsymbol{r}-\boldsymbol{r}_1)\right)^{\frac{3}{2}}} & \frac{(\boldsymbol{r}-\boldsymbol{r}_1)^{\mathsf{T}}}{\sqrt{(\boldsymbol{r}-\boldsymbol{r}_1)^{\mathsf{T}}(\boldsymbol{r}-\boldsymbol{r}_1)}} \\ \frac{(\boldsymbol{v}-\boldsymbol{v}_2)^{\mathsf{T}}}{\sqrt{(\boldsymbol{r}-\boldsymbol{r}_2)^{\mathsf{T}}(\boldsymbol{r}-\boldsymbol{r}_2)}} - \frac{(\boldsymbol{r}-\boldsymbol{r}_2)^{\mathsf{T}}(\boldsymbol{v}-\boldsymbol{v}_2)(\boldsymbol{r}-\boldsymbol{r}_2)^{\mathsf{T}}}{\left((\boldsymbol{r}-\boldsymbol{r}_2)^{\mathsf{T}}(\boldsymbol{r}-\boldsymbol{r}_2)\right)^{\frac{3}{2}}} & \frac{(\boldsymbol{r}-\boldsymbol{r}_2)^{\mathsf{T}}}{\sqrt{(\boldsymbol{r}-\boldsymbol{r}_2)^{\mathsf{T}}(\boldsymbol{r}-\boldsymbol{r}_2)}} \end{bmatrix} \tag{5}$$

The measurement vector and measurement Jacobian for the case of TDOA and FDOA measurements is shown below.

$$\boldsymbol{y} = \begin{bmatrix} \Delta r \\ \Delta\dot{r} \end{bmatrix} + \boldsymbol{w} \tag{6}$$

$$\boldsymbol{H} = \begin{bmatrix} \boldsymbol{H}_{\Delta r,r} & \boldsymbol{0} \\ \boldsymbol{H}_{\Delta\dot{r},r} & \boldsymbol{H}_{\Delta\dot{r},v} \end{bmatrix} \tag{7}$$

$$= \begin{bmatrix} \frac{(\boldsymbol{r}-\boldsymbol{r}_2)^{\mathsf{T}}}{\sqrt{(\boldsymbol{r}-\boldsymbol{r}_2)^{\mathsf{T}}(\boldsymbol{r}-\boldsymbol{r}_2)}} - \frac{(\boldsymbol{r}-\boldsymbol{r}_1)^{\mathsf{T}}}{\sqrt{(\boldsymbol{r}-\boldsymbol{r}_1)^{\mathsf{T}}(\boldsymbol{r}-\boldsymbol{r}_1)}} & \boldsymbol{0} \\ \frac{(\boldsymbol{v}-\boldsymbol{v}_2)^{\mathsf{T}}}{\sqrt{(\boldsymbol{r}-\boldsymbol{r}_2)^{\mathsf{T}}(\boldsymbol{r}-\boldsymbol{r}_2)}} - \frac{(\boldsymbol{r}-\boldsymbol{r}_2)^{\mathsf{T}}(\boldsymbol{v}-\boldsymbol{v}_2)(\boldsymbol{r}-\boldsymbol{r}_2)^{\mathsf{T}}}{\left((\boldsymbol{r}-\boldsymbol{r}_2)^{\mathsf{T}}(\boldsymbol{r}-\boldsymbol{r}_2)\right)^{\frac{3}{2}}} - \frac{(\boldsymbol{v}-\boldsymbol{v}_1)^{\mathsf{T}}}{\sqrt{(\boldsymbol{r}-\boldsymbol{r}_1)^{\mathsf{T}}(\boldsymbol{r}-\boldsymbol{r}_1)}} - \frac{(\boldsymbol{r}-\boldsymbol{r}_1)^{\mathsf{T}}(\boldsymbol{v}-\boldsymbol{v}_1)(\boldsymbol{r}-\boldsymbol{r}_1)^{\mathsf{T}}}{\left((\boldsymbol{r}-\boldsymbol{r}_1)^{\mathsf{T}}(\boldsymbol{r}-\boldsymbol{r}_1)\right)^{\frac{3}{2}}} & \frac{(\boldsymbol{r}-\boldsymbol{r}_2)^{\mathsf{T}}}{\sqrt{(\boldsymbol{r}-\boldsymbol{r}_2)^{\mathsf{T}}(\boldsymbol{r}-\boldsymbol{r}_2)}} - \frac{(\boldsymbol{r}-\boldsymbol{r}_1)^{\mathsf{T}}}{\sqrt{(\boldsymbol{r}-\boldsymbol{r}_1)^{\mathsf{T}}(\boldsymbol{r}-\boldsymbol{r}_1)}} \end{bmatrix}$$

Note that $\boldsymbol{H}_{\Delta r,r} = \boldsymbol{H}_{\Delta\dot{r},v}$. Evaluation of the state vector and measurement Jacobian would typically be performed with components in some inertial reference frame. But for convenience, they are shown here in tensor form. Given an initial set of measurements, the following section describes how the probability density function can be modeled as a uniform-Gaussian distribution, by first considering the simple case of linear measurements. The goal will then be to approximate the probability density of the orbital state using a Gaussian mixture.

3. UNDERDETERMINED MEASUREMENTS WITH GAUSSIAN NOISE

Consider a linear measurement system with a state $\boldsymbol{x} \in \mathbb{R}^n$, measurements $\boldsymbol{y} \in \mathbb{R}^m$, and measurement noise $\boldsymbol{w} \in \mathbb{R}^m$, where $m < n$.

$$\boldsymbol{y} = \boldsymbol{H}\boldsymbol{x} + \boldsymbol{w} \tag{8}$$

Let $\boldsymbol{w}$ obey a Gaussian probability distribution with zero mean and covariance $\boldsymbol{R}$.

$$p_w(\boldsymbol{w}) = |2\pi\boldsymbol{R}|^{-\frac{1}{2}} \exp\left(-\frac{1}{2}\boldsymbol{w}^{\mathsf{T}}\boldsymbol{R}^{-1}\boldsymbol{w}\right) \tag{9}$$

The matrix $\boldsymbol{H}$ is $m \times n$ with m independent rows. It has an m dimensional row space, $\mathbb{P}$, and an $(n-m)$-dimensional nullspace, $\mathbb{N}$. The state consists of two components: $\boldsymbol{x}_{\parallel} \in \mathbb{P}$ and $\boldsymbol{x}_{\perp} \in \mathbb{N}$.

$$\boldsymbol{x} = \boldsymbol{x}_{\parallel} + \boldsymbol{x}_{\perp} \tag{10}$$

The goal is now to describe the posterior probability density functions of $\boldsymbol{x}_{\parallel}$ and $\boldsymbol{x}_{\perp}$.

The value of $\boldsymbol{x}_{\perp}$ does not affect the measurement.

$$\boldsymbol{y} = \boldsymbol{H}\left(\boldsymbol{x}_{\parallel} + \boldsymbol{x}_{\perp}\right) + \boldsymbol{w} = \boldsymbol{H}\boldsymbol{x}_{\parallel} + \boldsymbol{w} \tag{11}$$

Therefore, the measurements do not provide any information on the distribution of $\boldsymbol{x}_{\perp}$. Instead, $\boldsymbol{x}_{\perp}$ can be assumed to have a uniform distribution over some subspace $\mathbb{A} \subset \mathbb{N}$.

$$p_{x_{\perp}}(\boldsymbol{x}_{\perp}) = \begin{cases} \frac{1}{\int_{\mathbb{A}} \mathrm{d}\boldsymbol{x}} & \text{if } \boldsymbol{x}_{\perp} \in \mathbb{A} \\ 0 & \text{if } \boldsymbol{x}_{\perp} \notin \mathbb{A} \end{cases} \tag{12}$$

Whereas $\boldsymbol{y}$ and $\boldsymbol{x}_{\parallel}$ have different dimensions, they are one-to-one. The solution for $\boldsymbol{x}_{\parallel}$ is given by the Moore-Penrose pseudoinverse, which is the minimum-norm solution that satisfies the measurements.

$$\boldsymbol{x}_{\parallel} = \boldsymbol{H}^{\mathsf{T}}(\boldsymbol{H}\boldsymbol{H}^{\mathsf{T}})^{-1}(\boldsymbol{y} - \boldsymbol{w}) \tag{13}$$

Clearly this solution lies in the row space of $\boldsymbol{H}$. To describe the probability density of $\boldsymbol{x}_{\parallel}$, the property that linear combinations of independent, Gaussian variables are also Gaussian can be used. Therefore, $\boldsymbol{x}_{\parallel}$ is Gaussian with mean $\boldsymbol{m}_{\parallel}$ and covariance $\boldsymbol{P}_{\parallel}$.

$$\boldsymbol{m}_{\parallel} = \boldsymbol{H}^{\mathsf{T}}(\boldsymbol{H}\boldsymbol{H}^{\mathsf{T}})^{-1}\boldsymbol{y} \tag{14}$$

$$\boldsymbol{P}_{\parallel} = \boldsymbol{H}^{\mathsf{T}}(\boldsymbol{H}\boldsymbol{H}^{\mathsf{T}})^{-1}\boldsymbol{R}(\boldsymbol{H}\boldsymbol{H}^{\mathsf{T}})^{-\mathsf{T}}\boldsymbol{H} \tag{15}$$

$$p_{x_{\parallel}}(\boldsymbol{x}_{\parallel}) = |2\pi\boldsymbol{P}_{\parallel}|^{-\frac{1}{2}} \exp\left(-\frac{1}{2}\left(\boldsymbol{x}_{\parallel} - \boldsymbol{m}_{\parallel}\right)^{\mathsf{T}}\boldsymbol{P}_{\parallel}^{-1}\left(\boldsymbol{x}_{\parallel} - \boldsymbol{m}_{\parallel}\right)\right) \tag{16}$$

Thus, the state can be modeled as a uniform-Guassian distribution, being uniform over $\mathbb{A}$ and being Gaussian along $\mathbb{P}$. To approximate this distribution with a GM, one approach is to create a grid of points in $\mathbb{A}$ and select a covariance, $\boldsymbol{P}_{\perp}$, with nonzero variances in $\mathbb{N}$ to model the uniform distribution over $\mathbb{A}$. The means of the Gaussian components are computed by adding $\boldsymbol{m}_{\parallel}$ to the grid point locations in $\mathbb{A}$. The covariances of the Gaussian components are computed by adding $\boldsymbol{P}_{\parallel}$ and $\boldsymbol{P}_{\perp}$.

For smooth, nonlinear measurements, $\boldsymbol{y} = \boldsymbol{h}(\boldsymbol{x}) + \boldsymbol{w}$, there is an $(n-m)$-dimension manifold that produces identical measurement values. The posterior probability density for $\boldsymbol{x}$ can be approximated as uniform-Gaussian, being uniform over this manifold and Gaussian along dimensions spanned by the Jacobian $\partial\boldsymbol{h}/\partial\boldsymbol{x}$. Approximation by GM can be performed by defining a mesh over the manifold, and selection of $\boldsymbol{P}_{\perp}$ with nonzero variances in the nullspace of the measurement Jacobian evaluated locally at each mesh point. The covariance $\boldsymbol{P}_{\parallel}$ can be computed at each mesh point also using the local evaluation of the measurement Jacobian. The means of the Gaussian components are defined at the mesh points, and the covariances of the Gaussian components are computed by adding $\boldsymbol{P}_{\parallel}$ and $\boldsymbol{P}_{\perp}$.

The following sections describe selection of means, variances in the nullspace, and weights given nonlinear measurements of the position and linear measurements of the velocity. The values are combined to consider the full orbital state along with the Gaussian distribution in the rowspace in Section 8.

4. GM APPROXIMATION OF UNIFORM DISTRIBUTION ON A CIRCLE

This section describes the GM approximation of a uniform distribution on a circle. This approximation will be used as a kernel for defining the GM approximation of a uniform distribution on a hyperboloid.

4.1 Background: GM Approximation of a Univariate Uniform Distribution

The use of GM approximations for probabilistic intial orbit determination was introduced by DeMars & Jah in Reference [11]. Based on angle and angular-rate observations of an object, their approach defined a constrained admissible region within the range and range-rate subspace. A uniform probability density over this region was approximated using a GM. This approximation of a univariate uniform distribution was used as a kernel to approximate the constrained admissible region by taking multiple slices of the two-dimensional subspace. The following assumptions for the GM were made:
1. The weights are equal for all components.
2. The means are evenly distributed across the support of the uniform distribution.
3. The Gaussian mixture is homoscedastic.
A condition was derived for the optimal standard deviation of the Gaussian components to minimize the L_2 distance between the uniform distribution and the GM approximation. This condition can be numerically solved. For example, for 10 components approximating a uniform distribution over $0 \leq x \leq 1$, the optimal standard deviation is 0.0696. The resulting GM approximation is illustrated in Fig. 1.

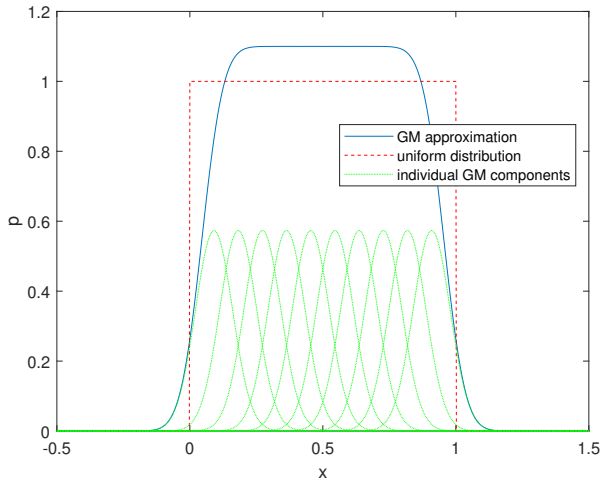

Fig. 1: Gaussian mixture approximation of a univariate uniform distribution

Before continuing, note that the constrained admissible region is the union of a one-dimensional manifold in position space and a one-dimensional manifold in velocity space. Each of these manifolds is linear in the Cartesian coordinates for position or velocity, respectively. Other measurement types can lead to manifolds that are curvilinear with respect to the Cartesian coordinates. Assembling GM approximations for uniform distributions over such manifolds is more challenging, particularly because the uniform distribution and the Gaussian components have different support.

4.2 Circular Distribution

Consider a uniform probability distribution over a circle with radius r. The circle can be parameterized by an angle θ whose probability density has a constant value of $1/(2\pi r)$ for all values of $\theta \in [0, 2\pi)$. This distribution will be approximated by a GM in Cartesian components, associated with a reference frame C. At each location on the circle define radial, $\hat{\boldsymbol{e}}_r$, and transverse, $\hat{\boldsymbol{e}}_\theta$, coordinate vectors.

$$[\hat{\boldsymbol{e}}_r]_C = \begin{bmatrix} \cos\theta \\ \sin\theta \end{bmatrix} \qquad [\hat{\boldsymbol{e}}_\theta]_C = \begin{bmatrix} -\sin\theta \\ \cos\theta \end{bmatrix} \tag{17}$$

Assume that the mean locations are located within the support of the uniform distribution, i.e. on the radius r circle. Further assume that all components have equal weight, $\alpha_l = 1/L$, and equal transverse spacing $\Delta\theta = 2\pi/L$.

$$\theta_l = \frac{2\pi(l-1)}{L} \tag{18}$$

$$[\boldsymbol{m}_l]_C = r \begin{bmatrix} \cos\theta_l \\ \sin\theta_l \end{bmatrix} \tag{19}$$

The covariances for all Gaussian components are related by rotations through $\Delta\theta$, with each Gaussian component having nonzero variance, σ_t^2, in the transverse direction, which is tangential to the circle. A schematic illustration of the GM is shown in Figure 2.

Alternative GMs could be considered where the means are located inside the circle, and with nonzero variances in the radial direction. Here, the placement of the means on the radius r circle is motivated by the intention for the orbit-determination problem to update the GM for additional measurements using a GM extended Kalman filter, as further described in a later section. (Variance in the radial direction would also be added to model a uniform-Gaussian distribution due to sensor noise in the circular measurement, but this component is neglected in this section.) Therefore the GM distribution can be defined by selecting σ_t.

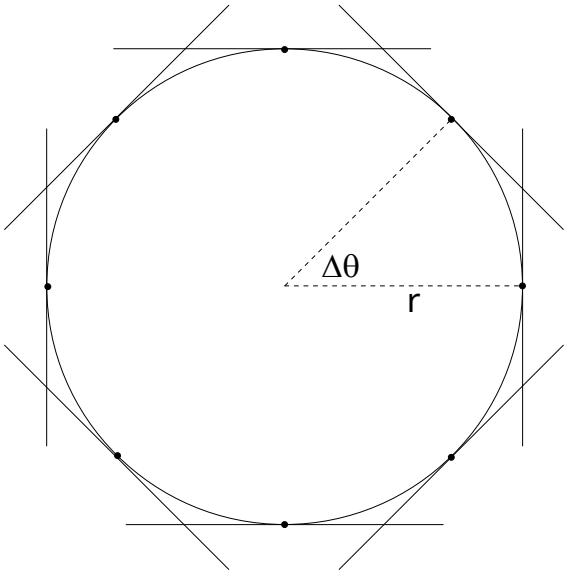

Fig. 2: Illustration of GM approximation of uniform distribution on a circle

In Reference [11], the L_2 distance between the univariate uniform distribution and the GM approximation was minimized. The "faceted" GM approximation chosen here has a different support than the targeted uniform distribution on a circle. The different supports of the distributions causes the evaluation of the L_2 distance to be challenging. Therefore an alternative condition for the variance value is chosen.

Because the value of σ_t is equal for all Gaussian components, the condition can be written in local radial and transverse coordinates, or without loss of generality, for a Gaussian component aligned with $\theta_l = 0$ so that x is in the radial direction and y is in the transverse direction. An approximation of uniformity along the radius r circle can be obtained by specifying that for each Gaussian component, the probability density at the mean is twice the probability density at the point of intersection with the neighboring Gaussian components.

$$\frac{1}{\sqrt{2\pi}\sigma_t}\exp\left\{-\frac{1}{2}\left(\frac{0}{\sigma_t}\right)^2\right\} = 2\frac{1}{\sqrt{2\pi}\sigma_t}\exp\left\{-\frac{1}{2}\left(\frac{r\tan\frac{\Delta\theta}{2}}{\sigma_t}\right)^2\right\} \tag{20}$$

$$\sigma_t^2 = \frac{\left(r\tan\frac{\Delta\theta}{2}\right)^2}{\ln 4} \tag{21}$$

Because the GM approximation uses Gaussian components with principal variances aligned with the local radial and transverse directions, the components will not overlap as smoothly as in the univariate case, illustrated in Figure 1. The GM approximation has local maxima at the mean of each Gaussian component and near the midpoint between adjacent components (where there is strong overlap in the probability density contributions). The selected uniformity approximation condition essentially attempts to balance the value of these local maxima. For a circle with $r = 1$ and $L = 10$, the solution for σ_t is 0.2344. By comparison, the GM approximation with 10 components for a univariate uniform distribution over a support of 2π results in an optimal standard deviation of 0.4372.

5. GM APPROXIMATION OF UNIFORM DISTRIBUTION ON A HYPERBOLA

Consider a uniform probability distribution over a portion of one branch of a hyperbola in a plane. Define a reference frame C with coordinate vectors $\hat{\boldsymbol{i}}$ pointing in the direction from receiver 2 to receiver 1 and $\hat{\boldsymbol{j}}$ orthogonal to $\hat{\boldsymbol{i}}$. The positions of the receivers relative to the midpoint between them have components of $[c\ 0]^\mathsf{T}$ and $[-c\ 0]^\mathsf{T}$. For an arbitrary location $[x\ y]^\mathsf{T}$, the ranges to each foci are given by the following.

$$r_{t,1} = \sqrt{(x-c)^2 + y^2} \tag{22}$$

$$r_{t,2} = \sqrt{(x+c)^2 + y^2} \tag{23}$$

The range difference is $\Delta r = r_{t,2} - r_{t,1}$. Without loss of generality, assume that $\Delta r \geq 0$.

For a given range difference, define the following parameters.

$$a = \frac{\Delta r}{2} \tag{24}$$

$$b = \sqrt{c^2 - a^2} \tag{25}$$

The locus of points that share that range difference is given by a hyperbola.

$$\frac{x^2}{a^2} - \frac{y^2}{b^2} = 1 \tag{26}$$

The hyperbola can be described by a parameter ψ.

$$x = a\cosh\psi \tag{27}$$

$$y = b\sinh\psi \tag{28}$$

The apex of the hyperbola is at $\psi = 0$. Locations along the asymptotes of the hyperbola are approached as ψ goes to infinity. (The value of ψ is equal to twice the area of the hyperbolic sector at x and y.)

At each location on the hyperbola, another local reference frame E can be defined with coordinate vectors $\hat{\boldsymbol{e}}_h$ tangential to the hyperbola (i.e. in the nullspace of the Δr measurement Jacobian) and $\hat{\boldsymbol{e}}_n$ normal to the hyperbola (i.e. in the rowspace of the Δr measurement Jacobian).

$$\begin{aligned}
\hat{\boldsymbol{e}}_n &= \frac{-\boldsymbol{H}_{\Delta r,r}^\mathsf{T}}{\sqrt{\boldsymbol{H}_{\Delta r,r}\boldsymbol{H}_{\Delta r,r}^\mathsf{T}}} \\
&= \frac{\frac{\boldsymbol{r}-\boldsymbol{r}_1}{\sqrt{(\boldsymbol{r}-\boldsymbol{r}_1)^\mathsf{T}(\boldsymbol{r}-\boldsymbol{r}_1)}} - \frac{\boldsymbol{r}-\boldsymbol{r}_2}{\sqrt{(\boldsymbol{r}-\boldsymbol{r}_2)^\mathsf{T}(\boldsymbol{r}-\boldsymbol{r}_2)}}}{\sqrt{\left(\frac{\boldsymbol{r}-\boldsymbol{r}_1}{\sqrt{(\boldsymbol{r}-\boldsymbol{r}_1)^\mathsf{T}(\boldsymbol{r}-\boldsymbol{r}_1)}} - \frac{\boldsymbol{r}-\boldsymbol{r}_2}{\sqrt{(\boldsymbol{r}-\boldsymbol{r}_2)^\mathsf{T}(\boldsymbol{r}-\boldsymbol{r}_2)}}\right)^\mathsf{T}\left(\frac{\boldsymbol{r}-\boldsymbol{r}_1}{\sqrt{(\boldsymbol{r}-\boldsymbol{r}_1)^\mathsf{T}(\boldsymbol{r}-\boldsymbol{r}_1)}} - \frac{\boldsymbol{r}-\boldsymbol{r}_2}{\sqrt{(\boldsymbol{r}-\boldsymbol{r}_2)^\mathsf{T}(\boldsymbol{r}-\boldsymbol{r}_2)}}\right)}} \\
&= \frac{\frac{\boldsymbol{r}-\boldsymbol{r}_1}{\sqrt{(\boldsymbol{r}-\boldsymbol{r}_1)^\mathsf{T}(\boldsymbol{r}-\boldsymbol{r}_1)}} - \frac{\boldsymbol{r}-\boldsymbol{r}_2}{\sqrt{(\boldsymbol{r}-\boldsymbol{r}_2)^\mathsf{T}(\boldsymbol{r}-\boldsymbol{r}_2)}}}{\sqrt{2 - 2\frac{(\boldsymbol{r}-\boldsymbol{r}_1)^\mathsf{T}(\boldsymbol{r}-\boldsymbol{r}_2)}{\sqrt{(\boldsymbol{r}-\boldsymbol{r}_1)^\mathsf{T}(\boldsymbol{r}-\boldsymbol{r}_1)}\sqrt{(\boldsymbol{r}-\boldsymbol{r}_2)^\mathsf{T}(\boldsymbol{r}-\boldsymbol{r}_2)}}}}
\end{aligned} \tag{29}$$

$$\hat{\boldsymbol{e}}_h = \frac{\frac{\boldsymbol{r}-\boldsymbol{r}_1}{\sqrt{(\boldsymbol{r}-\boldsymbol{r}_1)^{\mathsf{T}}(\boldsymbol{r}-\boldsymbol{r}_1)}} + \frac{\boldsymbol{r}-\boldsymbol{r}_2}{\sqrt{(\boldsymbol{r}-\boldsymbol{r}_2)^{\mathsf{T}}(\boldsymbol{r}-\boldsymbol{r}_2)}}}{\sqrt{\left(\frac{\boldsymbol{r}-\boldsymbol{r}_1}{\sqrt{(\boldsymbol{r}-\boldsymbol{r}_1)^{\mathsf{T}}(\boldsymbol{r}-\boldsymbol{r}_1)}} + \frac{\boldsymbol{r}-\boldsymbol{r}_2}{\sqrt{(\boldsymbol{r}-\boldsymbol{r}_2)^{\mathsf{T}}(\boldsymbol{r}-\boldsymbol{r}_2)}}\right)^{\mathsf{T}}\left(\frac{\boldsymbol{r}-\boldsymbol{r}_1}{\sqrt{(\boldsymbol{r}-\boldsymbol{r}_1)^{\mathsf{T}}(\boldsymbol{r}-\boldsymbol{r}_1)}} + \frac{\boldsymbol{r}-\boldsymbol{r}_2}{\sqrt{(\boldsymbol{r}-\boldsymbol{r}_2)^{\mathsf{T}}(\boldsymbol{r}-\boldsymbol{r}_2)}}\right)}} \tag{30}$$
$$= \frac{\frac{\boldsymbol{r}-\boldsymbol{r}_1}{\sqrt{(\boldsymbol{r}-\boldsymbol{r}_1)^{\mathsf{T}}(\boldsymbol{r}-\boldsymbol{r}_1)}} + \frac{\boldsymbol{r}-\boldsymbol{r}_2}{\sqrt{(\boldsymbol{r}-\boldsymbol{r}_2)^{\mathsf{T}}(\boldsymbol{r}-\boldsymbol{r}_2)}}}{\sqrt{2+2\frac{(\boldsymbol{r}-\boldsymbol{r}_1)^{\mathsf{T}}(\boldsymbol{r}-\boldsymbol{r}_2)}{\sqrt{(\boldsymbol{r}-\boldsymbol{r}_1)^{\mathsf{T}}(\boldsymbol{r}-\boldsymbol{r}_1)}\sqrt{(\boldsymbol{r}-\boldsymbol{r}_2)^{\mathsf{T}}(\boldsymbol{r}-\boldsymbol{r}_2)}}}}$$

The target probability distribution is uniform over the portion of the hyperbola from $\psi_{\min} \geq 0$ to some $\psi_{\max}$. The Gaussian mixture approximation of this distribution uses L components. Reference points on the hyperbola are defined, separated by equal step $\Delta\psi$ of the parameter.

$$\Delta\psi = \frac{\psi_{\max} - \psi_{\min}}{L+1} \tag{31}$$

$$\psi_l = \psi_{\min} + l\Delta\psi \tag{32}$$

The mean locations, $\boldsymbol{r}_l = [x_l\ y_l]^{\mathsf{T}}$, are computed by evaluating Eqs. (27) and (28) at ψ_l. The equal steps of $\Delta\psi$ place the means closer together near the apex of the hyperbola, and further apart near the asymptote of the hyperbola. This is attractive to provide the GM greater resolution in the region of the hyperbola with smaller radius of curvature.

The principal components of the covariance of each Gaussian component will be aligned with the tangential and normal directions at the reference point. The unit vectors along the tangential direction can be formed by taking derivatives of x and y with respect to ψ.

$$x' = a\sinh\psi \tag{33}$$

$$y' = b\cosh\psi \tag{34}$$

$$[\hat{\boldsymbol{e}}_h]_C = \frac{1}{\sqrt{(x')^2+(y')^2}}\begin{bmatrix} x' \\ y' \end{bmatrix} = \frac{1}{\sqrt{a^2\sinh^2\psi + b^2\cosh^2\psi}}\begin{bmatrix} a\sinh\psi \\ b\cosh\psi \end{bmatrix} \tag{35}$$

The unit vector in the normal direction is orthogonal to the tangential unit vector.

$$[\hat{\boldsymbol{e}}_n]_C = \frac{1}{\sqrt{a^2\sinh^2\psi + b^2\cosh^2\psi}}\begin{bmatrix} -b\cosh\psi \\ a\sinh\psi \end{bmatrix} \tag{36}$$

The standard deviation along the tangential direction is defined using a localized version of the Gaussian mixture approximation of a uniform distribution on a circle. The local radius of curvature at the reference point and the angular spacing to the neighboring reference points is used to evaluate the parameters for the approximation of a circular distribution. Evaluating the radius of curvature also requires the second derivatives of x and y.

$$x'' = a\cosh\psi \tag{37}$$

$$y'' = b\sinh\psi \tag{38}$$

$$\rho = \left|\frac{\left((x')^2+(y')^2\right)^{\frac{3}{2}}}{x'y''-y'x''}\right| = \left|\frac{\left(a^2\sinh^2\psi + b^2\cosh^2\psi\right)^{\frac{3}{2}}}{ab\sinh^2\psi - ab\cosh^2\psi}\right| = \frac{1}{ab}\left(a^2\sinh^2\psi + b^2\cosh^2\psi\right)^{\frac{3}{2}} \tag{39}$$

This expression defines the radius of curvature anywhere on the hyperbola. The radii of curvature at the reference points, ρ_l, are computed by evaluation at ψ_l.

The arclength, s, from the apex to any point on the hyperbola is given by the following.

$$\mathrm{gd}\,\psi = \mathrm{atan}(\sinh\psi) \tag{40}$$

$$s(\psi) = b\left(F\left(\mathrm{gd}\,\psi\middle|-\frac{a^2}{b^2}\right) - E\left(\mathrm{gd}\,\psi\middle|-\frac{a^2}{b^2}\right) + \sqrt{1+\frac{a^2}{b^2}\tanh\psi}\sinh\psi\right) \tag{41}$$

Here, gd is the Gudermannian function, F is the incomplete elliptic integral of the first kind, and E is the incomplete elliptic integral of the second kind. The arclength to each reference point as well as the points on the hyperbola at $\psi_{\min}$ and $\psi_{\max}$ are evaluated.

$$s_0 = s(\psi_{\min}) \tag{42}$$

$$s_l = s(\psi_l) \text{ for } l = 1, \ldots, L \tag{43}$$

$$s_{L+1} = s(\psi_{\max}) \tag{44}$$

The angular spacing used in the local circular approximation is evaluated from the arc lengths between neighboring mean locations and the local radius of curvature.

$$\Delta\theta_l = \frac{s_{l+1} - s_{l-1}}{2\rho_l} \text{ for } l = 1, \ldots, L \tag{45}$$

For each Gaussian component, the values of ρ_l and $\Delta\theta_l$ are used in Eq. (21) to evaluate σ_t^2, and is here labeled $\sigma_{h,l}^2$. Because the GM is not homoscedactic, certain components are intended to approximate larger regions of the uniform distribution than other components. Thus, the weight for each component is selected to scale the probability densities of each component at that component's mean to be equal.

$$\alpha_l = \frac{\sigma_{t,l}}{\sum_{k=1}^{L} \sigma_{t,k}} \tag{46}$$

6. GM APPROXIMATION ON A HYPERBOLOID

Augment the reference frame C with a third coordinate vector $\hat{\boldsymbol{k}} = \hat{\boldsymbol{i}} \times \hat{\boldsymbol{j}}$. Consider receiver locations $[\boldsymbol{r}_1]_C = [c\ 0\ 0]^\mathsf{T}$ and $[\boldsymbol{r}_2]_C = [-c\ 0\ 0]^\mathsf{T}$. For an arbitrary location $[x\ y\ z]^\mathsf{T}$, the ranges to each foci are given by the following.

$$r_{t,1} = \sqrt{(x-c)^2 + y^2 + z^2} \tag{47}$$

$$r_{t,2} = \sqrt{(x+c)^2 + y^2 + z^2} \tag{48}$$

The range difference is $\Delta r = r_{t,2} - r_{t,1}$. Without loss of generality, assume that $\Delta r \geq 0$. For a given range difference, the generating hyperbola has parameters a and b defined in Eqs. (24) and (25).

The GM approximation of a uniform distribution over a hyperboloid is constructed by combining the GM approximations of uniform distributions over a hyperbola and a circle. Mean locations are defined in a mesh along the generating hyperbola and the circle of revolution about the axis of symmetry of the hyperboloid. The number of mean locations along the generating hyperbola is L_h, and the number of mean locations along the circle of revolution is L_c. Steps of $\Delta\psi$ along the generating hyperbola are used as described in Eqs. (31) and (32), replacing L with L_h in Eq. (31). Steps of $\Delta\theta$ along the circle of revolution are used as described in Eq. (18), replacing L with L_c. The resulting mean locations are given by the following.

$$[\boldsymbol{r}_{ij}]_C = \begin{bmatrix} a\cosh\psi_i \\ b\sinh\psi_i\cos\theta_j \\ b\sinh\psi_i\sin\theta_j \end{bmatrix} \quad \text{for } i = 1, \ldots, L_h \text{ and } j = 1, \ldots, L_c \tag{49}$$

Augment the reference frame E with a third coordinate vector $\hat{\boldsymbol{e}}_c = \hat{\boldsymbol{e}}_h \times \hat{\boldsymbol{e}}_n$, which is tangential to the circle of revolution (and lies in the nullspace of the Δr measurement Jacobian). The local coordinate vectors can be expressed in components of the C frame.

$$[\hat{\boldsymbol{e}}_h]_C = \frac{1}{\sqrt{a^2\sinh^2\psi + b^2\cosh^2\psi}} \begin{bmatrix} a\sinh\psi \\ b\cosh\psi\cos\theta \\ b\cosh\psi\sin\theta \end{bmatrix} \tag{50}$$

$$[\hat{\boldsymbol{e}}_c]_C = \begin{bmatrix} 0 \\ -\sin\theta \\ \cos\theta \end{bmatrix} \tag{51}$$

$$[\hat{\boldsymbol{e}}_n]_C = \frac{1}{\sqrt{a^2\sinh^2\psi + b^2\cosh^2\psi}} \begin{bmatrix} -b\cosh\psi \\ a\sinh\psi\cos\theta \\ a\sinh\psi\sin\theta \end{bmatrix} \tag{52}$$

The values of $\hat{\boldsymbol{e}}_{h,ij}$, $\hat{\boldsymbol{e}}_{c,j}$, and $\hat{\boldsymbol{e}}_{n,ij}$ are found by evaluation at the corresponding values of ψ_i and θ_j.

For each value of ψ_i, the approximation on a hyperbola is evaluated using the local radius of curvature and the spacing between neighboring values of ψ_i. The value of $\sigma_{h,i}$ is computed as described in Section 5. For each value of ψ_i, the approximation on a circle is evaluated using the radius of the circle of revolution, $b\sinh\psi_i$, and the spacing of $\Delta\theta$. The value of σ_t is computed as described in Section 4, and is here labeled as $\sigma_{c,i}$.

$$\boldsymbol{P}_{\perp\Delta r,ij} = \begin{bmatrix} \hat{\boldsymbol{e}}_{h,ij} & \hat{\boldsymbol{e}}_{c,j} \end{bmatrix} \begin{bmatrix} \sigma_{h,i}^2 & 0 \\ 0 & \sigma_{c,i}^2 \end{bmatrix} \begin{bmatrix} \hat{\boldsymbol{e}}_{h,ij}^{\mathsf{T}} \\ \hat{\boldsymbol{e}}_{c,j}^{\mathsf{T}} \end{bmatrix} \tag{53}$$

Similar to the GM approximation for a hyperbola, the weights are selected to equalize the probability density contribution of each Gaussian component at that component's mean.

$$\alpha_{ij} = \frac{\sigma_{h,i}\sigma_{c,i}}{L_c \sum_{i=1}^{L_h} \sigma_{h,i}\sigma_{c,i}} \tag{54}$$

7. GM APPROXIMATION OF FREQUENCY MEASUREMENTS

For a given transmitter position, the FOA measurements provide two conditions for the three components of the transmitter's velocity, or the FDOA measurements provide a single condition. This section describes GM approximation for the resulting uniform-Gaussian distribution in velocity space. These are conditions on the velocity components in the plane of the relative positions from the transmitter to each receiver, which is the $\hat{\boldsymbol{e}}_h\hat{\boldsymbol{e}}_n$ plane. In particular, for a given transmitter position, the frequency measurements become nonhomogeneous linear equations for the transmitter velocity. The approach described in Section 3 can be combined with the univariate GM reviewed in Section 4.1 to develop the GM approximation.

The FOA measurements can be rewritten as follows.

$$\begin{bmatrix} \dot{r}_{t,1} \\ \dot{r}_{t,2} \end{bmatrix} = \begin{bmatrix} \frac{(\boldsymbol{r}_{ij}-\boldsymbol{r}_1)^{\mathsf{T}}}{\sqrt{(\boldsymbol{r}_{ij}-\boldsymbol{r}_1)^{\mathsf{T}}(\boldsymbol{r}_{ij}-\boldsymbol{r}_1)}} \\ \frac{(\boldsymbol{r}_{ij}-\boldsymbol{r}_2)^{\mathsf{T}}}{\sqrt{(\boldsymbol{r}_{ij}-\boldsymbol{r}_2)^{\mathsf{T}}(\boldsymbol{r}_{ij}-\boldsymbol{r}_2)}} \end{bmatrix} \boldsymbol{v} - \begin{bmatrix} \frac{(\boldsymbol{r}_{ij}-\boldsymbol{r}_1)^{\mathsf{T}}\boldsymbol{v}_1}{\sqrt{(\boldsymbol{r}_{ij}-\boldsymbol{r}_1)^{\mathsf{T}}(\boldsymbol{r}_{ij}-\boldsymbol{r}_1)}} \\ \frac{(\boldsymbol{r}_{ij}-\boldsymbol{r}_2)^{\mathsf{T}}\boldsymbol{v}_2}{\sqrt{(\boldsymbol{r}_{ij}-\boldsymbol{r}_2)^{\mathsf{T}}(\boldsymbol{r}_{ij}-\boldsymbol{r}_2)}} \end{bmatrix} \tag{55}$$

$$\begin{bmatrix} \frac{(\boldsymbol{r}_{ij}-\boldsymbol{r}_1)^{\mathsf{T}}}{\sqrt{(\boldsymbol{r}_{ij}-\boldsymbol{r}_1)^{\mathsf{T}}(\boldsymbol{r}_{ij}-\boldsymbol{r}_1)}} \\ \frac{(\boldsymbol{r}_{ij}-\boldsymbol{r}_2)^{\mathsf{T}}}{\sqrt{(\boldsymbol{r}_{ij}-\boldsymbol{r}_2)^{\mathsf{T}}(\boldsymbol{r}_{ij}-\boldsymbol{r}_2)}} \end{bmatrix} \boldsymbol{v} = \begin{bmatrix} \dot{r}_{t,1} \\ \dot{r}_{t,2} \end{bmatrix} + \begin{bmatrix} \frac{(\boldsymbol{r}_{ij}-\boldsymbol{r}_1)^{\mathsf{T}}\boldsymbol{v}_1}{\sqrt{(\boldsymbol{r}_{ij}-\boldsymbol{r}_1)^{\mathsf{T}}(\boldsymbol{r}_{ij}-\boldsymbol{r}_1)}} \\ \frac{(\boldsymbol{r}_{ij}-\boldsymbol{r}_2)^{\mathsf{T}}\boldsymbol{v}_2}{\sqrt{(\boldsymbol{r}_{ij}-\boldsymbol{r}_2)^{\mathsf{T}}(\boldsymbol{r}_{ij}-\boldsymbol{r}_2)}} \end{bmatrix} \tag{56}$$

$$\boldsymbol{b} \equiv \begin{bmatrix} \dot{r}_{t,1} \\ \dot{r}_{t,2} \end{bmatrix} + \begin{bmatrix} \frac{(\boldsymbol{r}_{ij}-\boldsymbol{r}_1)^{\mathsf{T}}\boldsymbol{v}_1}{\sqrt{(\boldsymbol{r}_{ij}-\boldsymbol{r}_1)^{\mathsf{T}}(\boldsymbol{r}_{ij}-\boldsymbol{r}_1)}} \\ \frac{(\boldsymbol{r}_{ij}-\boldsymbol{r}_2)^{\mathsf{T}}\boldsymbol{v}_2}{\sqrt{(\boldsymbol{r}_{ij}-\boldsymbol{r}_2)^{\mathsf{T}}(\boldsymbol{r}_{ij}-\boldsymbol{r}_2)}} \end{bmatrix} \tag{57}$$

The unique solution for the component of $\boldsymbol{v}$ lying in the plane of the relative positions is labeled $\boldsymbol{v}_{\|}$ and is given by the Moore-Penrose pseudoinverse.

$$\boldsymbol{v}_{\|} = \boldsymbol{H}_{\dot{r},v}^{\mathsf{T}} \left(\boldsymbol{H}_{\dot{r},v}\boldsymbol{H}_{\dot{r},v}^{\mathsf{T}}\right)^{-1} \boldsymbol{b} \tag{58}$$

The velocity component in the $\hat{\boldsymbol{e}}_c$ direction does not affect the FOA measurements. Therefore, the probability distribution along the $\hat{\boldsymbol{e}}_c$ velocity component is uniform within some some bound $v_{c,\max}$.

$$p_{v_c}(v_c) = \begin{cases} \frac{1}{2v_{c,\max}} & v_c \in [-v_{c,\max}, v_{c,\max}] \\ 0 & v_c \notin [-v_{c,\max}, v_{c,\max}] \end{cases} \tag{59}$$

This uniform distribution is approximated with a GM with L_v components using the approach developed in [11], and summarized in Section 4.1. The mean values are given by the following.

$$v_{c,k} = -v_{c,\max} + \frac{2v_{c,\max}k}{L_v+1} \qquad \text{for } k = 1,\ldots,L_v \tag{60}$$

$$\boldsymbol{v}_k = \boldsymbol{v}_{\parallel} + v_{c,k}\hat{\boldsymbol{e}}_c \tag{61}$$

The standard deviation σ_v is evaluated numerically.

$$\boldsymbol{P}_{\perp\dot{r}} = \sigma_v^2 \hat{\boldsymbol{e}}_c \hat{\boldsymbol{e}}_c^{\mathsf{T}} \tag{62}$$

The FDOA measurement can be similarly manipulated.

$$\Delta\dot{r} = \left(\frac{(\boldsymbol{r}-\boldsymbol{r}_2)^{\mathsf{T}}}{\sqrt{(\boldsymbol{r}-\boldsymbol{r}_2)^{\mathsf{T}}(\boldsymbol{r}-\boldsymbol{r}_2)}} - \frac{(\boldsymbol{r}-\boldsymbol{r}_1)^{\mathsf{T}}}{\sqrt{(\boldsymbol{r}-\boldsymbol{r}_1)^{\mathsf{T}}(\boldsymbol{r}-\boldsymbol{r}_1)}} \right) \boldsymbol{v} - \left(\frac{(\boldsymbol{r}-\boldsymbol{r}_2)^{\mathsf{T}}\boldsymbol{v}_2}{\sqrt{(\boldsymbol{r}-\boldsymbol{r}_2)^{\mathsf{T}}(\boldsymbol{r}-\boldsymbol{r}_2)}} - \frac{(\boldsymbol{r}-\boldsymbol{r}_1)^{\mathsf{T}}\boldsymbol{v}_1}{\sqrt{(\boldsymbol{r}-\boldsymbol{r}_1)^{\mathsf{T}}(\boldsymbol{r}-\boldsymbol{r}_1)}} \right) \tag{63}$$

$$\left(\frac{(\boldsymbol{r}-\boldsymbol{r}_2)^{\mathsf{T}}}{\sqrt{(\boldsymbol{r}-\boldsymbol{r}_2)^{\mathsf{T}}(\boldsymbol{r}-\boldsymbol{r}_2)}} - \frac{(\boldsymbol{r}-\boldsymbol{r}_1)^{\mathsf{T}}}{\sqrt{(\boldsymbol{r}-\boldsymbol{r}_1)^{\mathsf{T}}(\boldsymbol{r}-\boldsymbol{r}_1)}} \right) \boldsymbol{v} = \Delta\dot{r} + \frac{(\boldsymbol{r}-\boldsymbol{r}_2)^{\mathsf{T}}\boldsymbol{v}_2}{\sqrt{(\boldsymbol{r}-\boldsymbol{r}_2)^{\mathsf{T}}(\boldsymbol{r}-\boldsymbol{r}_2)}} - \frac{(\boldsymbol{r}-\boldsymbol{r}_1)^{\mathsf{T}}\boldsymbol{v}_1}{\sqrt{(\boldsymbol{r}-\boldsymbol{r}_1)^{\mathsf{T}}(\boldsymbol{r}-\boldsymbol{r}_1)}} \tag{64}$$

$$b = \Delta\dot{r} + \frac{(\boldsymbol{r}-\boldsymbol{r}_2)^{\mathsf{T}}\boldsymbol{v}_2}{\sqrt{(\boldsymbol{r}-\boldsymbol{r}_2)^{\mathsf{T}}(\boldsymbol{r}-\boldsymbol{r}_2)}} - \frac{(\boldsymbol{r}-\boldsymbol{r}_1)^{\mathsf{T}}\boldsymbol{v}_1}{\sqrt{(\boldsymbol{r}-\boldsymbol{r}_1)^{\mathsf{T}}(\boldsymbol{r}-\boldsymbol{r}_1)}} \tag{65}$$

Note that only the component of the transmitter's velocity in the direction equal to the difference in the relative position unit vectors affects the TDOA measurement. The solution for this velocity component is again given by the Moore-Penrose pseudoinverse.

$$\boldsymbol{v}_{\parallel} = \boldsymbol{H}_{\Delta\dot{r},v}^{\mathsf{T}} \frac{b}{\boldsymbol{H}_{\Delta\dot{r},v}\boldsymbol{H}_{\Delta\dot{r},v}^{\mathsf{T}}} \tag{66}$$

The solution for $\boldsymbol{v}_{\parallel}$ lies in the row space of $\boldsymbol{H}_{\Delta\dot{r},v} = \boldsymbol{H}_{\Delta r,r}$, which is the same direction as $\hat{\boldsymbol{e}}_n$.

Velocity components in the $\hat{\boldsymbol{e}}_h$ and $\hat{\boldsymbol{e}}_c$ directions do not affect the FDOA measurement. Therefore, the probability distribution of the velocity is uniform in the $\hat{\boldsymbol{e}}_h\hat{\boldsymbol{e}}_c$ plane within some some bound $v_{\max}$.

$$p_{v_h,v_c}(v_h,v_c) = \begin{cases} \frac{1}{4v_{\max}^2} & (v_h \in [-v_{\max}, v_{\max}]) \wedge (v_c \in [-v_{\max}, v_{\max}]) \\ 0 & \text{otherwise} \end{cases} \tag{67}$$

This uniform distribution is approximated with a Gaussian mixture with L_v^2 components. The mean velocities are distributed on a grid on the $\hat{\boldsymbol{e}}_h\hat{\boldsymbol{e}}_c$ plane.

$$v_{h,i} = -v_{\max} + \frac{2v_{\max} i}{L_v + 1} \qquad \text{for } i = 1, \ldots, L_v \tag{68}$$

$$v_{c,j} = -v_{\max} + \frac{2v_{\max} j}{L_v + 1} \qquad \text{for } j = 1, \ldots, L_v \tag{69}$$

$$\boldsymbol{v}_{ij} = \boldsymbol{v}_{\parallel} + v_{h,i}\hat{\boldsymbol{e}}_h + v_{c,j}\hat{\boldsymbol{e}}_c \tag{70}$$

The standard deviation σ_v is evaluated numerically, and each Gaussian component is assigned a covariance matrix with this standard deviation in principal directions of $\hat{\boldsymbol{e}}_h$ and $\hat{\boldsymbol{e}}_c$.

$$\boldsymbol{P}_{\perp\Delta\dot{r}} = \sigma_v^2 \left(\hat{\boldsymbol{e}}_c \hat{\boldsymbol{e}}_c^{\mathsf{T}} + \hat{\boldsymbol{e}}_h \hat{\boldsymbol{e}}_h^{\mathsf{T}} \right) \tag{71}$$

8. GM APPROXIMATION OF THE ORBITAL STATE

For the posterior distribution of the orbital state given a set of TDOA and FOA measurements, there is a three-dimensional manifold of the state space that satifies the measurements and over which the distribution is uniform. To develop a GM approximation of the posterior distribution, a mesh of mean locations must be constructed over this manifold, and covariances must be selected to approximate the uniform distribution.

The previous sections described the GM approximation of a TDOA hyperboloid in position space, and for a given position, the velocity components undetermined by the frequency measurements. But given a set of TDOA and frequency measurements it is desired to describe the uniform-Gaussian distribution in the full orbital state space.

The means for this GM approximation will be concatenations of the mean positions on the TDOA hyperboloid and mean velocities satisfying the frequency measurements. These mean states form a mesh spaced along the generating hyperboloid and circle of rotation in position space and along the undetermined velocity components. For FOA measurements, the total number of components is $N = L_h L_c L_v$, and components are here notated with i as the index along the generating hyperbola, j as the index along the circle of revolution, and k as the index along the velocity component in the $\hat{\boldsymbol{e}}_c$ direction. The mean states are written as follows.

$$\boldsymbol{m}_{ijk} = \begin{bmatrix} \boldsymbol{r}_{ij} \\ \boldsymbol{v}_{\parallel,ij} + v_{c,k}\hat{\boldsymbol{e}}_{c,j} \end{bmatrix} \tag{72}$$

Here, $\boldsymbol{r}_{ij}$ was defined in Eq. (49). For FDOA measurements, the total number of components is $N = L_h L_c L_v^2$, and l is the additional index along the velocity component in the $\hat{\boldsymbol{e}}_h$ direction. The mean states are shown below.

$$\boldsymbol{m}_{ijkl} = \begin{bmatrix} \boldsymbol{r}_{ij} \\ \boldsymbol{v}_{\parallel,ij} + v_{c,k}\hat{\boldsymbol{e}}_{c,j} + v_{h,l}\hat{\boldsymbol{e}}_{h,ij} \end{bmatrix} \tag{73}$$

The GM approximation of a circle and of a univariate variable provided guidance for sizing the desired variances along the mesh directions. But the requirement for the covariance components that approximate the uniform aspects of the distribution is that they should span the nullspace of the Jacobian of the full measurement vector (i.e. TDOA and frequency measurements) with respect to the full state vector (i.e. position and velocity components).

The covariances of the Gaussian components in the nullspace of the measurement Jacobian, $\boldsymbol{H}$, approximate the uniform distribution. One direction in the nullspace has zero position components and velocity components along the $\hat{\boldsymbol{e}}_c$ direction. Therefore, the variance σ_v^2 can be associated with this direction. The covariance $\boldsymbol{P}_{\perp\Delta r,ij}$ defined in Eq. (53) was designed to approximate a uniform distribution over the TDOA hyperboloid. Whereas a variation $\delta\boldsymbol{r}$ in position over the hyperboloid produces no change in the TDOA measurement, variation in position along $\hat{\boldsymbol{e}}_h$ without a corresponding variation $\delta\boldsymbol{v}$ in velocity will produce a change in the FOA measurements. (This is precisely the same reason that the solution for $\boldsymbol{v}_\parallel$ is a function of $\boldsymbol{r}$).

Define $\boldsymbol{H}_{ijk}$ as the evaluation of $\boldsymbol{H}$ at the mean state $\boldsymbol{m}_{ijk}$. The solution for the covariance in the velocity components and the covariance between the position and velocity to associated with the position variance will be illustrated here for the case of FOA measurements. To construct additional components of the nullspace of $\boldsymbol{H}_{ijk}$, it will be convenient to define $\boldsymbol{H}_{\dot{r}r,ijk}$ as the lower-left 2×3 partition, and $\boldsymbol{H}_{\dot{r}v,ijk}$ as the lower-right 2×3 partition.

$$\boldsymbol{H}_{\dot{r}r,ijk}\delta\boldsymbol{r} + \boldsymbol{H}_{\dot{r}v,ijk}\delta\boldsymbol{v} = \boldsymbol{0} \tag{74}$$

Given a deviation $\delta\boldsymbol{r}$ the solution for the deviation $\delta\boldsymbol{v}$ in the rowspace of $\boldsymbol{H}_{\dot{r}v,ijk}$ is given by the Moore-Penrose pseudoinverse.

$$\delta\boldsymbol{v} = -\boldsymbol{H}_{\dot{r}v,ijk}^{\mathsf{T}}\left(\boldsymbol{H}_{\dot{r}v,ijk}\boldsymbol{H}_{\dot{r}v,ijk}^{\mathsf{T}}\right)^{-1}\boldsymbol{H}_{\dot{r}r,ijk}\delta\boldsymbol{r} \tag{75}$$

This solution can be used to find the velocity covariance to associate with the position covariance, and the cross covariance between them.

$$\mathrm{E}\left\{\delta\boldsymbol{v}\delta\boldsymbol{v}^{\mathsf{T}}\right\} = \mathrm{E}\left\{\boldsymbol{H}_{\dot{r}v,ijk}^{\mathsf{T}}\left(\boldsymbol{H}_{\dot{r}v,ijk}\boldsymbol{H}_{\dot{r}v,ijk}^{\mathsf{T}}\right)^{-1}\boldsymbol{H}_{\dot{r}r,ijk}\delta\boldsymbol{r}\delta\boldsymbol{r}^{\mathsf{T}}\boldsymbol{H}_{\dot{r}r,ijk}^{\mathsf{T}}\left(\boldsymbol{H}_{\dot{r}v,ijk}\boldsymbol{H}_{\dot{r}v,ijk}^{\mathsf{T}}\right)^{-T}\boldsymbol{H}_{\dot{r}v,ijk}\right\} \tag{76}$$

$$\boldsymbol{P}_{v,ijk} = \boldsymbol{H}_{\dot{r}v,ijk}^{\mathsf{T}}\left(\boldsymbol{H}_{\dot{r}v,ijk}\boldsymbol{H}_{\dot{r}v,ijk}^{\mathsf{T}}\right)^{-1}\boldsymbol{H}_{\dot{r}r,ijk}\boldsymbol{P}_{\perp\Delta r,ij}\boldsymbol{H}_{\dot{r}r,ijk}^{\mathsf{T}}\left(\boldsymbol{H}_{\dot{r}v,ijk}\boldsymbol{H}_{\dot{r}v,ijk}^{\mathsf{T}}\right)^{-T}\boldsymbol{H}_{\dot{r}v,ijk} \tag{77}$$

$$\mathrm{E}\left\{\delta\boldsymbol{r}\delta\boldsymbol{v}^{\mathsf{T}}\right\} = \mathrm{E}\left\{-\delta\boldsymbol{r}\delta\boldsymbol{r}^{\mathsf{T}}\boldsymbol{H}_{\dot{r}r,ijk}^{\mathsf{T}}\left(\boldsymbol{H}_{\dot{r}v,ijk}\boldsymbol{H}_{\dot{r}v,ijk}^{\mathsf{T}}\right)^{-T}\boldsymbol{H}_{\dot{r}v,ijk}\right\} \tag{78}$$

$$\boldsymbol{P}_{rv,ijk} = -\boldsymbol{P}_{\perp\Delta r,ij}\boldsymbol{H}_{\dot{r}r,ijk}^{\mathsf{T}}\left(\boldsymbol{H}_{\dot{r}v,ijk}\boldsymbol{H}_{\dot{r}v,ijk}^{\mathsf{T}}\right)^{-T}\boldsymbol{H}_{\dot{r}v,ijk} \tag{79}$$

The solution for the case of an FDOA measurement is similar, using the associated partitions of the measurement Jacobian evaluate at $\boldsymbol{m}_{ijkl}$.

With this, the covariance components modeling the uniform distribution can be assembled. For the case of FOA measurements, the covariance matrix has the following form.

$$\boldsymbol{P}_{\perp,ijk} = \begin{bmatrix} \boldsymbol{P}_{\perp\Delta r,ij} & \boldsymbol{P}_{rv,ijk} \\ \boldsymbol{P}_{rv,ijk}^{\mathsf{T}} & \boldsymbol{P}_{v,ijk} \end{bmatrix} + \begin{bmatrix} \boldsymbol{0} & \boldsymbol{0} \\ \boldsymbol{0} & \boldsymbol{P}_{\perp\dot{r},j} \end{bmatrix} \tag{80}$$

For an FDOA measurement, the covariance matrix is shown below.

$$\boldsymbol{P}_{\perp,ijkl} = \begin{bmatrix} \boldsymbol{P}_{\perp\Delta r,ij} & \boldsymbol{P}_{rv,ijkl} \\ \boldsymbol{P}_{rv,ijkl}^{\mathsf{T}} & \boldsymbol{P}_{v,ijkl} \end{bmatrix} + \begin{bmatrix} \boldsymbol{0} & \boldsymbol{0} \\ \boldsymbol{0} & \boldsymbol{P}_{\perp\Delta\dot{r},ij} \end{bmatrix} \tag{81}$$

For the GM described in the previous section, and its corresponding covariance values, was designed to approximate the uniform distribution over the manifold satisfying the TDOA and FOA measurements. To account for the Gaussian distribution in the directions orthogonal to this manifold due to measurement noise, additional components must be added to the state covariance. As described in Section 3, this state covariance is related to the measurement noise covariance by the Moore-Penrose pseudoinverse of the measurement Jacobian.

The value $\boldsymbol{H}_{ijk}$ is the evaluation of $\boldsymbol{H}$ at the mean position and velocity of the (i,j,k)th Gaussian component. The covariance for each component due to measurement noise is given by the following for the case of FOA measurements.

$$\boldsymbol{R} = \begin{bmatrix} \sigma_{\Delta r}^2 & 0 & 0 \\ 0 & \sigma_{\dot{r},1}^2 & 0 \\ 0 & 0 & \sigma_{\dot{r},2}^2 \end{bmatrix} \tag{82}$$

For an FDOA measurement, the measurement noise covariance matrix is shown below.

$$\boldsymbol{R} = \begin{bmatrix} \sigma_{\Delta r}^2 & 0 \\ 0 & \sigma_{\Delta\dot{r}}^2 \end{bmatrix} \tag{83}$$

$$\boldsymbol{P}_{\parallel,ijk} = \boldsymbol{H}_{ijk}^{\mathsf{T}}(\boldsymbol{H}_{ijk}\boldsymbol{H}_{ijk}^{\mathsf{T}})^{-1}\boldsymbol{R}(\boldsymbol{H}_{ijk}\boldsymbol{H}_{ijk}^{\mathsf{T}})^{-\mathsf{T}}\boldsymbol{H}_{ijk} \tag{84}$$

The total covariance for each component is the sum of the covariance approximating the dimensions with uniform distribution and the contribution due to sensor noise.

$$\boldsymbol{P}_{ijk} = \boldsymbol{P}_{\perp,ijk} + \boldsymbol{P}_{\parallel,ijk} \tag{85}$$

Lastly, the weight of each Gaussian component is computed. For FOA measurements, the weight of the (i,j,k)th component is shown below.

$$\alpha_{ijk} = \frac{\sqrt{|\boldsymbol{P}_{ijk}|}}{\sum_{i=1}^{L_h}\sum_{j=1}^{L_c}\sum_{k=1}^{L_v}\sqrt{|\boldsymbol{P}_{ijk}|}} \tag{86}$$

For an FDOA measurement, the weight of the (i,j,k,l)th component is similar.

$$\alpha_{ijkl} = \frac{\sqrt{|\boldsymbol{P}_{ijkl}|}}{\sum_{i=1}^{L_h}\sum_{j=1}^{L_c}\sum_{k=1}^{L_v}\sum_{l=1}^{L_v}\sqrt{|\boldsymbol{P}_{ijkl}|}} \tag{87}$$

9. GM EXTENDED KALMAN FILTER

The preceding sections described the initialization of a GM using a set of TDOA and frequency measurements. The propagation of the GM and update of the GM from subsequent measurements can be performed using a GM extended Kalman filter. In the propagation step, the nonlinear orbital dynamics are modeled using a selected propagator, subject to process noise.

$$\dot{\boldsymbol{x}} = \begin{bmatrix} \boldsymbol{v} \\ \boldsymbol{f}(\boldsymbol{x}) \end{bmatrix} + \begin{bmatrix} \boldsymbol{0} \\ \boldsymbol{I} \end{bmatrix} \boldsymbol{u} \tag{88}$$

Here the process noise $\boldsymbol{u}$ is assumed to be Gaussian with spectral density $\boldsymbol{Q}$.

$$\mathrm{E}\{\boldsymbol{u}(t)\boldsymbol{u}^{\mathsf{T}}(\tau)\} = \boldsymbol{Q}\delta(t-\tau) \tag{89}$$

The mean values are propagated from time t_k to t_{k+1} by numerical solution of the noise-free dynamic model.

$$\dot{\boldsymbol{x}}_i = \begin{bmatrix} \boldsymbol{v}_i \\ \boldsymbol{f}(\boldsymbol{x}_i) \end{bmatrix} \qquad \text{for } i = 1,\ldots,N \tag{90}$$

The covariance matrices are propagated using the state-transition matrix $\boldsymbol{\Phi}_i(t_{k+1},t_k)$ evaluated along the associated mean value.

$$\boldsymbol{P}_i(t_{k+1}) = \boldsymbol{\Phi}_i(t_{k+1},t_k)\boldsymbol{P}_i(t_k)\boldsymbol{\Phi}_i^{\mathsf{T}}(t_{k+1},t_k) + \int_{t_k}^{t_{k+1}} \boldsymbol{\Phi}_i(t_{k+1},\tau) \begin{bmatrix} \boldsymbol{0} \\ \boldsymbol{I} \end{bmatrix} \boldsymbol{Q} \begin{bmatrix} \boldsymbol{0} & \boldsymbol{I} \end{bmatrix} \boldsymbol{\Phi}_i^{\mathsf{T}}(t_{k+1},\tau)\mathrm{d}\tau \qquad \text{for } i = 1,\ldots,N \tag{91}$$

The update step is performed when measurements are received. The measurement Jacobian is evaluated at each mean state, and notated as $\boldsymbol{H}_i$.

$$\boldsymbol{K}_i = \boldsymbol{P}_i^- \boldsymbol{H}_i^{\mathsf{T}} \left(\boldsymbol{H}_i \boldsymbol{P}_i^- \boldsymbol{H}_i^{\mathsf{T}} + \boldsymbol{R}\right)^{-1} \tag{92}$$

The Kalman gain is used to update the means and covariances, with the prior values notated with a superscript $-$ and the posterior values notated with a superscript $+$.

$$\boldsymbol{x}_i^+ = \boldsymbol{x}_i^- + \boldsymbol{K}_i \left(\boldsymbol{y} - \boldsymbol{h}(\boldsymbol{x}_i^-)\right) \tag{93}$$

$$\boldsymbol{P}_i^+ = \left(\boldsymbol{I} - \boldsymbol{K}_i \boldsymbol{H}_i\right) \boldsymbol{P}_i^- \tag{94}$$

The evaluation of the measurement residuals at the mean states is the motivation, mentioned in an earlier section, for initializing the GM with states that satisfy the initial measurements. The weights are updated using the measurement likelihood given the posterior means and covariances.

$$\omega_i = \frac{1}{\sqrt{\left|2\pi \left(\boldsymbol{H}_i^+ \boldsymbol{P}_i^+ \boldsymbol{H}_i^{+\mathsf{T}} + \boldsymbol{R}\right)\right|}} \exp\left(-\frac{1}{2} \left(\boldsymbol{y} - \boldsymbol{h}(\boldsymbol{x}_i^+)\right)^{\mathsf{T}} \left(\boldsymbol{H}_i^+ \boldsymbol{P}_i^+ \boldsymbol{H}_i^{+\mathsf{T}} + \boldsymbol{R}\right)^{-1} \left(\boldsymbol{y} - \boldsymbol{h}(\boldsymbol{x}_i^+)\right)\right) \tag{95}$$

Here, $\boldsymbol{H}_i^+$ is the evaluation of the measurement Jacobian at $\boldsymbol{x}_i^+$.

$$w_i^+ = \frac{\omega_i w_i}{\sum_{k=1}^N \omega_k w_k} \tag{96}$$

Note that the propagation of the covariances depend on linearization of the dynamics (via the state-transition matrix), and the update of the means and covariances depend on linearization of the measurement model (via the measurement Jacobian). Both linearizations are evaluated at the mean. Approximation of uniform-Gaussian distributions with highly accurate measurements using a small number of GM components will result in covariance matrices with high "aspect ratio", i.e. small covariances in the row space of the measurement Jacobian and large covariances in the nullspace. Components with large differences in the variance magnitudes are sensitive to roundoff error. This roundoff error can be somewhat alleviated by using a square-root implementation of the extended Kalman filter.

However, components of this type are also particularly sensitive to linearization error. Components with large aspect ratios are being used to approximate a large portion of the uniform distribution. The linearization evaluated at the component's mean may not be a good approximation over this entire portion. Specifically, the Gaussian components were initially constructed with large variances in the nullspace of the measurement Jacobian. But linearized propagation and update of the covariance means that linearization error may result in projections of these components erroneously falling in the rowspace of the measurement Jacobian when evaluated at future mean values. These errors can cause large updates to these components, which essentially opens up probability-density gaps in the mesh of Gaussian components approximating the original uniform-Guassian distribution. To alleviate these linearization errors, nonlinear filtering techniques could be applied to covariance update. Alternatively, sufficient Gaussian components can be used so that the eigenvalues of the covariance matrices are all similar magnitudes. Therefore, a high resolution GM may be needed to reduce linearization error in the filtering of highly accurate measurements, but at increased computational expense.

10. EXAMPLE RESULTS

The GMEKF is illustrated here using passive RF measurements of a transmitting object by a pair of receiver satellites. All three satellites are simulated as obeying Keplerian orbits about the Earth with 7000 km semimajor axis. The two receivers are in circular, equatorial orbits offset from each other by 1 deg of true anomaly. The transmitting object has an eccentricity of 0.01, inclination of 1 deg, and is offset by an additional degree in true anomaly.

The GM for the transmitter's orbital state was created by simulating time-difference of arrival between the receivers and frequency of arrival measurements at each receiver, which correspond to the range difference from the transmitter to the receivers and the range rate from the transmitter to each receiver. RF measurements are simulated once per minute starting at an initial time of $t = 0$. The simulated measurements included Gaussian noise of 0.1 km in the range difference and 0.001 km/s in the range rates. The GM used 27,000 components.

An illustration of the GM during the search campaign is shown in Figure 3. Figure 3(a) shows the initial GM, and Figures 3(b-f) show the posterior GM after each subsequent RF measurement. For each subfigure, the transmitter's and receivers' positions are shown in Earth-centered inertial coordinates, with the green square indicating the transmitter and green $\times$ indicating the receiver. For each component of the GM, the 2σ ellipsoid of the marginal probability density function for the position components is shown, with shading proportional to the product of the component weight and the probability density evaluated at the mean location.

The approximation of the TDOA hyperboloid is apparent in the initial GM. In the final distribution, the probability density has collapsed to two small regions, each of which looks like it could be reasonably approximated as Gaussian. The GM appears to effectively describe the complex geometry as the probability density evolves from the initial to the final distribution.

11. CONCLUSION

An initial set of TDOA and frequency measurements results in a uniform-Gaussian distribution for the transmitter's orbital state, with uniform distribution over a manifold with complicated geometry. This paper presented a method to initialize a GM approximation of this distribution. Using this GM, subsequent RF measurements can be incorporated via a GM extended Kalman filter.

The GM characterizes the probability density of the transmitter's orbital state from the first detection. This approach contrasts to other common techniques for initial orbit determination, which wait until sufficient measurements have been collected so that the probability density function can be approximated as a single component. The characterization of the probability density during the early stages after detection has the potential to speed up other responses to the detection, such as cueing a follow-on sensor to search for the transmitter.

REFERENCES

[1] Arie Yeredor and Eyal Angel. Joint TDOA and FDOA estimation: A conditional bound and its use for optimally weighted localization. *IEEE Transactions on Signal Processing*, 59(4):1612–1623, 2011.

[2] Edwin G W Peters, Timothy Bateman, Rabbia Saleem, Melrose Brown, and Andrew Lambert. A software defined radio based method for accurate frequency estimation for space domain awareness in real-time. In *AMOS Conference*, 2022.

[3] Y.T. Chan and K.C. Ho. A simple and efficient estimator for hyperbolic location. *IEEE Transactions on Signal Processing*, 42(8):1905–1915, 1994.

[4] Tim Pattison and S. I. Chou. Sensitivity analysis of dual-satellite geolocation. *IEEE Transactions on Aerospace and Electronic Systems*, 36(1):56–71, 2000.

[5] Jeff Mason. Algebraic two-satellite TOA/FOA position solution on an ellipsoidal earth. *IEEE Transactions on Aerospace and Electronic Systems*, 40(3):1087–1092, 2004.

[6] Darko Mušicki, Regina Kuane, and Wolfgang Koch. Mobile emitter geolocation and tracking using TDOA and FDOA measurements. *IEEE Transactions on Signal Processing*, 58(3):1863–1874, 2010.

[7] L. A. Romero and Jeff Mason. Evaluation of direct and iterative methods for overdetermined systems of TOA geolocation equations. *IEEE Transactions on Aerospace and Electronic Systems*, 47(2):1213–1229, 2011.

[8] Richard S. Hujsak, James W. Woodburn, and John H. Seago. The Orbit Determination Tool Kit (ODTK) - Version 5. *Advances in the Astronautical Sciences*, 127:381–400, 2007.

[9] Simon Shuster, Andrew J. Sinclair, and T. Alan Lovell. Initial relative-orbit determination using heterogeneous TDOA. In *IEEE Aerospace Conference Proceedings*, 2017.

[10] Troy A. Henderson, Yasmeen Hack, Sophia Sunkin, T. Alan Lovell, Joshuah Hess, and Jessica Wightman. Initial Relative-Orbit Determination of Space Objects Via Radio Frequency Signal Localization. In *AAS/AIAA Astrodynamics Specialist Conference*, 2020.

[11] Kyle J. DeMars and Moriba K. Jah. Probabilistic initial orbit determination using Gaussian mixture models. *Journal of Guidance, Control, and Dynamics*, 36(5):1324–1335, 2013.

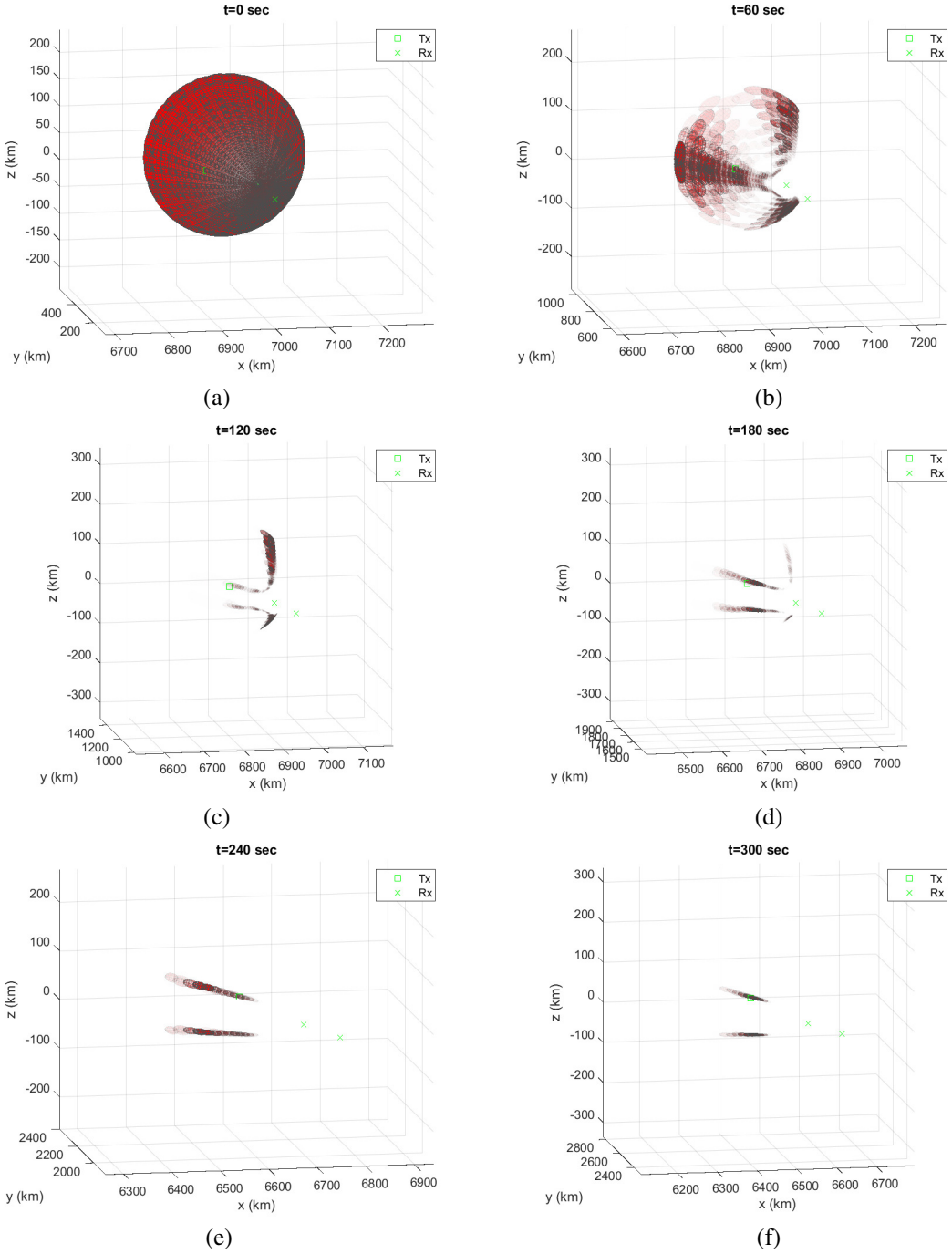

Fig. 3: Illustration of GM EKF